A forebrain organoid model of progranulin-associated frontotemporal dementia

Sophie Goldsmith [1], Gustavo Morrone Barbat Parfitt [1], Adriana Cunha [1] Matthew Gegg [2],

Aitana Sogorb Esteve [3,4], Jonathon D. Rohrer [4], Selina Wray [1]

1 Department of Neurodegenerative Disease, Queen Square Institute of Neurology, University College London, 2 Clinical and Movement Neurosciences, University College London. 3 UK Dementia Research Institute at University College London, 4 Dementia Research Centre, Queen Square Institute of Neurology, University College London

Background

Heterozygous mutations in *GRN,* leading to haploinsufficiency of the progranulin (PGRN) protein, cause TDP-43 pathology at post-mortem. *GRN*-FTD accounts for approximately 5-10% of FTD cases. However, little is currently known about the link between the reduction in PGRN and the accumulation of TDP-43 aggregates in neurons. PGRN is often found co-localised with LAMP1 and plays a key role in homeostatic lysosome function, including enzyme maturity and activity. Homozygous *GRN* mutations have been linked with neuronal ceroid lipofuscinosis (NCL), a lysosomal storage disorder, further emphasising PGRN's role in the lysosome. PGRN is highly expressed in microglia, and several recent studies have highlighted potential non-cell autonomous mechanisms underpinning PGRN-FTD. Therefore, our aim is to establish forebrain organoid, microglia, and co-culture models of PGRN-FTD to further investigate and characterise TDP-43 pathology and lysosomal dysfunction.

Methods

Isogenic induced pluripotent stem cell (iPSC) lines engineered to harbour the *GRN R493X* mutation (homozygous and heterozygous) in the Kolf2.1J background were obtained from the iNDI initiative. (1).

Forebrain organoids were differentiated from iPSCs using a protocol adapted from Pasca et al, 2015, (2)). Embryoid bodies (EBs) were formed using $1.5x10^5$ live cells/ml and were then maintained and fed in 96-well v-bottom plates using a series of medias. The base media was N2B27 without vitamin A for the first 70 days and then with vitamin A after (Day 2-8: XAV939 (2uM) + SB431542 (10uM) + LDN193189 (100nM), Day 8-24: FGFb (20ng/ml) + EGF (20ng/ml), Day 24-70: BDNF (20ng/ml), Day 70+ vitamin A was included).

iPSC-derived microglia like cells (iMGs) were differentiated using a protocol adapted from Garcia-Reitboeck et al. (2018) and Xiang et al. (2018), (3,4). In brief, EBs were generated from iPSCs, using $1x10^5$ live cells/ml. After 4 days, EBs were transferred to T75 flasks and maintained on myeloid media (X-Vivo 15 media with 100ng/ml MCSF and 25ng/ml IL3). Each week, myeloid progenitor cells were harvested and plated at a density of $5x10^5$ / well of a 6-well plate in maturation media (DMEM F-12 media with 100ng/ml IL34, 25ng/ml MCSF and 5ng/ml TGFβ1) for 2 weeks.

Successful differentiation in our organoid and microglia models was confirmed by immunocytochemistry (ICC). Characterisation of TDP-43 and lysosomal phenotypes is ongoing.

Results

Forebrain Organoid Model

Forebrain organoids were generated using the protocol above and whole mount immunocytochemistry at 30DIV was performed. Successful staining with PAX6 and Nestin and clear rosette formation confirmed successful neuronal differentiation in our lines. For the whole mount we used Sunjin Lab RapiClear 1.52 Solution (RC152002) (*see Figure 1).*

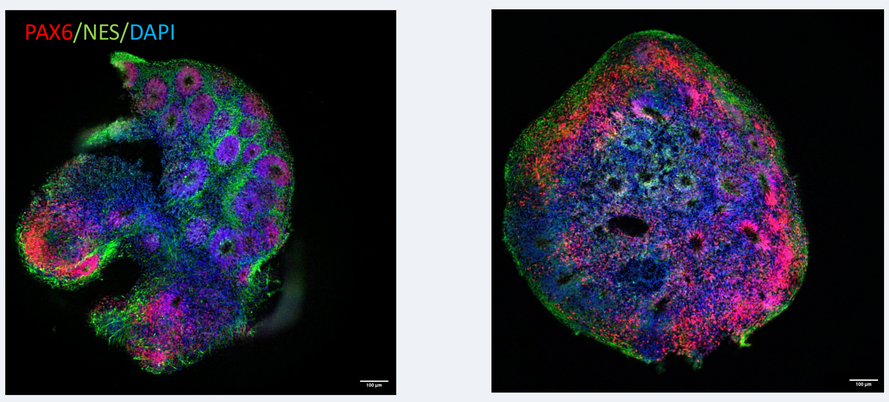

WT/WT bottom plane

R493X/R439X mid plane

Figure 1. To confirm successful neuronal differentiation and the presence of neural progenitor cells, whole mount immunocytochemistry was performed on organoids at 30 DIV. Two images are shown as examples of sections taken during quality checking. DAPI (blue), Nestin (green) and PAX6 (red). Scale bars show 100µm.

Characterising TDP-43 phenotypes in organoid model

After confirming successful differentiation, we next characterised TDP-43 levels, specifically protein expression using western blot. As seen in Figure 2, there is a trending, step-wise increase in full length TDP-43 (43kDa) and a band at 35kDa, assumed to be a fragment of TDP-43 at 100DIV. This increase in the 35kDa protein then becomes significant at 180DIV in *R493X/R493X* organoids compared to WT controls.

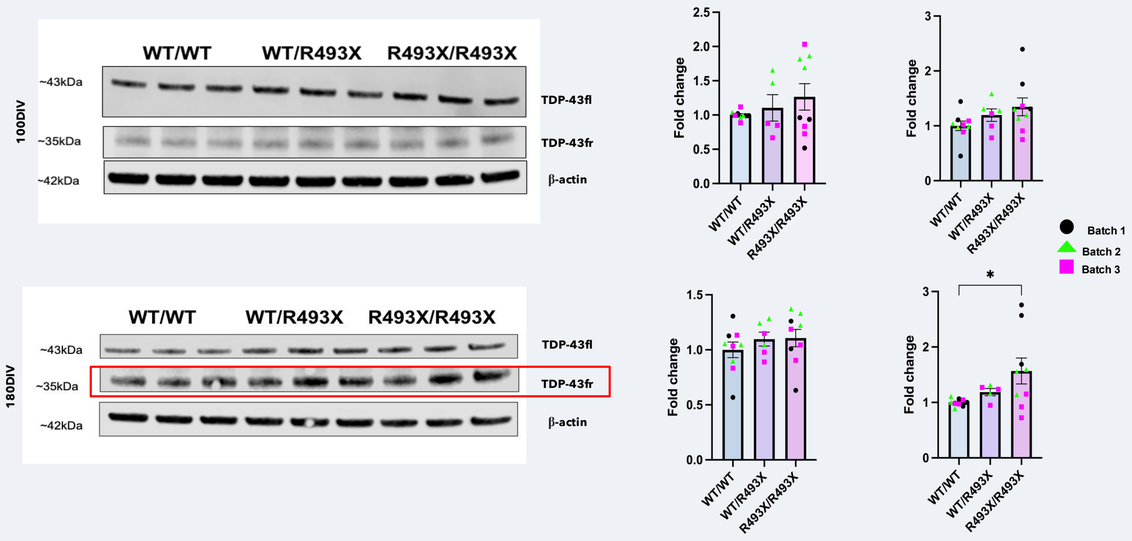

Figure 2. Western blot of *WT/WT, WT/R493X,* and *R493X/R493X* forebrain organoids at 100DIV (top) and 180DIV (bottom), probed for TDP-43 (polyclonal Ab) and β-actin as a loading control. Quantification of TDP-43 full length (43kDa) expression, normalised to loading control at 100DIV (top) and 180DIV (bottom) Quantification of TDP-43 35kDa band expression, normalised to loading control at 100DIV (top) and 180DIV (bottom). Fold change for figures calculated from average of WT controls (n=3) on each blot. Each data point represents one organoid, refer to key for batches. One-way ANOVAs were performed *P<0.05, Data is displayed as mean ± SEM.

Characterising lysosomal phenotypes in organoid model

We next investigated lysosomal dysfunction within our organoids. Firstly, using ICC, we found an increase in LAMP1 expression in our *R493X/R493X* models compared with controls (see Figure 3). On top of this, we carried out lysosomal enzyme activity assays for glucocerebrosidase (GCase), Hexosaminidase (Hex) and Beta-galactosidase (β-gal) as functional measures of the lysosome. As can be seen in Figure 4, GCase and Hex activity is trending upwards in a stepwise manner between *WT/WT, WT/R493X* and *R493X/R493X* and β-gal activity is significantly increased in *R493X/R493X* compared to controls.

Results

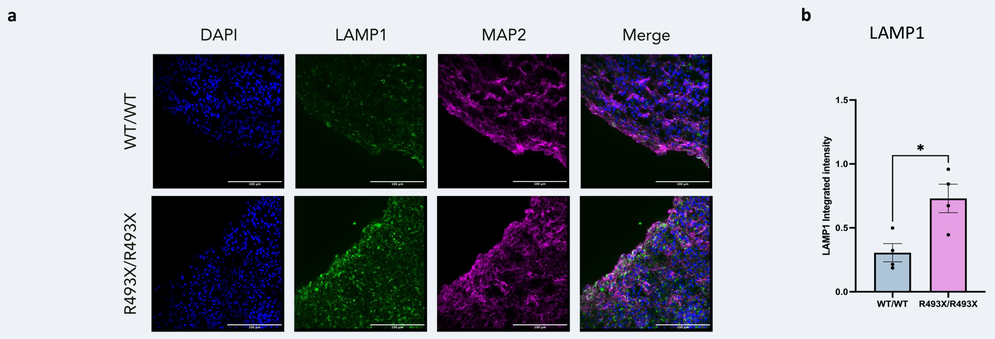

Figure 3. a) ICC to investigate LAMP1 in 180DIV *WT/WT and R493X/R493X* in forebrain organoid sections. Organoids were stained with MAP2 (magenta), LAMP1 (green). Merge image shows LAMP1, MAP2 and DAPI composite image. The scale bars show 100µm. (100x magnification). b) graph showing quantification of LAMP1 integrated intensity. Unpaired two-tailed t-tests were performed *P<0.05. Data is displayed as mean ± SEM.

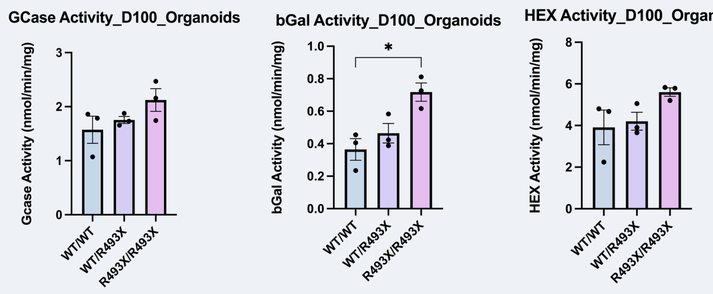

Figure 4. Lysosomal enzyme activity assays for GCase, β-gal and Hex in organoid lysates. Each point represents one organoid. Data is displayed as mean ± SEM.

iPSC-derived microglia

Microglia were characterised using ICC for Iba1 and TREM2. This confirmed successful differentiation.

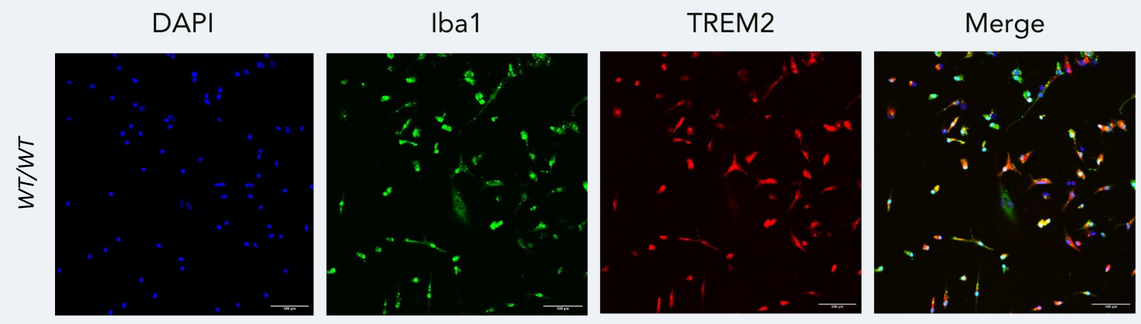

Figure 4. Characterisation of iPSC-derived microglia (iMGs) using immunocytochemistry. IMGs were stained with DAPI (blue), Iba1 (green) and TREM2 (red) to confirm microglial like identity. Scale bars show 100µm.

Characterising lysosomal phenotypes in microglia model

We investigated lysosomal function in microglia using the same assays previously used in organoids. We carried out ICC for LAMP1 as well as lysosomal enzyme activity assays. Our results showed a trending increase in LAMP1 expression in our *R493X/R493X* compared with controls (see Figure 5). Additionally, GCase activity was trending downwards, whilst β-gal and Hex were trending upwards in our *GRN* models indicating potential lysosome dysfunction (see Figure 6).

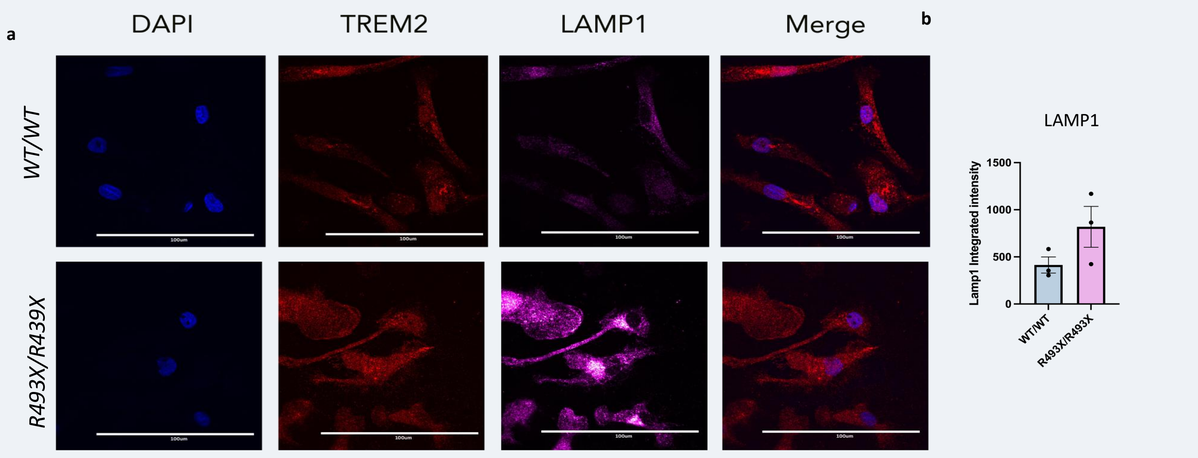

Figure 5. (a) ICC to investigate lysosomal phenotypes in WT and *R493X* homozygous microglia. Microglia were stained with TREM2 (red) and LAMP1 (magenta). Merge image shows TREM2 and DAPI composite image. The scale bars show 100µm. (100x magnification). (b) graph showing quantification of LAMP1 integrated intensity. Data is displayed as mean ± SEM.

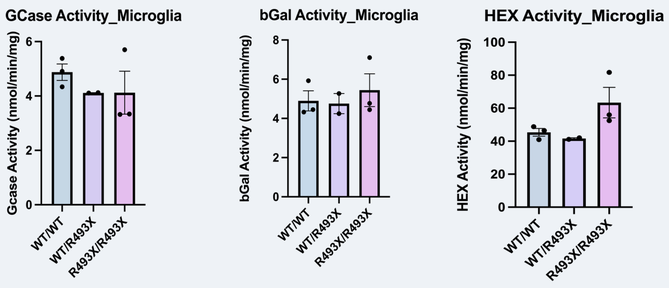

Figure 6. Lysosomal enzyme activity assays for GCase, β-gal and Hex in microglia lysates. Each point represents one sample. Data is displayed as mean ± SEM.

Conclusion

We have successfully established and characterised both an iPSC-derived forebrain organoid and microglia model of GRN-FTD. Our data indicates a stepwise change in the TDP-43 35kDa band in 180DIV organoids with the difference being significant between *WT/WT* and *R493X/R493X* organoids. We are currently investigating whether this is a cleaved fragment or a splice variant, otherwise known a short-TDP-43. Additionally, we show some lysosomal phenotypes with LAMP1 protein expression being upregulated in *R493X/R493X* in both microglia and organoids compared with controls and preliminary lysosomal enzyme activity assays indicating potential lysosome dysregulation in both models. Our next steps are to optimise a co-culture model of forebrain organoids and microglia in a mix-match approach and continue to characterise TDP-43 and lysosomal phenotypes.

Acknowledgements: SG is funded by the Familial Frontotemporal Dementia Studentship, the National Brain Appeal.

References: (1) Ramos, D. M., Skarnes, W. C., Singleton, A. B., et al. (2021) Tackling neurodegenerative diseases with genomic engineering: A new stem cell initiative from the NIH. Neuron, 109, 1080– 1083 (2) Paşca, A.M., Sloan, S.A., Clarke, L.E., Tian, Y., Makinson, C.D., Huber, N., Kim, C.H., Park, J.Y., O'rourke, N.A., Nguyen, K.D. and Smith, S.J., 2015. Functional cortical neurons and astrocytes from human pluripotent stem cells in 3D culture. Nature methods, 12(7), pp.671-678. (3) Garcia-Reitboeck, P., Phillips, A., Piers, T.M., Villegas-Llerena, C., Butler, M., Mallach, A., Rodrigues, C., Arber, C.E., Heslegrave, A., Zetterberg, H. and Neumann, H., 2018. Human induced pluripotent stem cell-derived microglia-like cells harboring TREM2 missense mutations show specific deficits in phagocytosis. Cell Reports, 24(9), pp.2300-2311. (4) Xiang, X., Piers, T.M., Wefers, B., Zhu, K., Mallach, A., Brunner, B., Kleinberger, G., Song, W., Colonna, M., Herms, J. and Wurst, W., 2018. The Trem2 R47H Alzheimer's risk variant impairs splicing and reduces Trem2 mRNA and protein in mice but not in humans. Molecular neurodegeneration, 13, pp.1-14. (5) Sung, W., Noh, M.Y., Nahm, M., Kim, Y.S., Ki, C.S., Kim, Y.E., Kim, H.J. and Kim, S.H., 2024. Progranulin haploinsufficiency mediates cytoplasmic TDP-43 aggregation with lysosomal abnormalities in human microglia. Journal of Neuroinflammation, 21(1), pp.1-20. (6) Mohan, S., Sampognaro, P.J., Argouarch, A.R., Maynard, J.C., Welch, M., Patwardhan, A., Courtney, E.C., Zhang, J., Mason, A., Li, K.H. and Huang, E.J., 2021. Processing of progranulin into granulins involves multiple lysosomal proteases and is affected in frontotemporal lobar degeneration. Molecular neurodegeneration, 16(1), p.51. (7) Herskowitz, J.H., Gozal, Y.M., Duong, D.M., Dammer, E.B., Gearing, M., Ye, K., Lah, J.J., Peng, J., Levey, A.I. and Seyfried, N.T., 2012. Asparaginyl endopeptidase cleaves TDP-43 in brain. Proteomics, 12(15-16), pp.2455-2463.